ADVANCES IN NUCLEAR SCIENCE AND APPLICATIONS

Volume 1, No. 3 (2025), P. 162-178

Cluster structure of the Borromean nucleus ^{9}Be and its astrophysical relevance

K.O. Mendibayev[1,2,*], S.M. Lukyanov[1]

[1]Joint Institute for Nuclear Research, Dubna, Russia

[2]Institute of Nuclear Physics, Almaty, Kazakhstan

e-mail: kayrat1988@bk.ru

DOI: 10.63907/ansa.v1i3.54
Received: 29 August 2025

Abstract

The study of cluster structures in light nuclei has become a central direction in modern nuclear physics. Experimental and theoretical investigations have revealed that many light systems, such as ^{6}He, ^{8}Be, ^{12}C, and others, exhibit pronounced cluster configurations that strongly influence reaction mechanisms. Particularly striking is the α-cluster structure of ^{12}C and its excited Hoyle state, which plays a key role in astrophysical nucleosynthesis. Among light nuclei, the stable yet weakly bound ^{9}Be nucleus is of special interest due to its Borromean character and competing cluster configurations, typically described as $(\alpha+\alpha+n)$ or $(^{5}\mathrm{He}+\alpha)$. These structural features manifest themselves in decay channels, scattering processes, and transfer reactions, and they directly affect the cross sections relevant for astrophysical scenarios such as the triple-α process and the r-process. The paper provides a comprehensive overview of theoretical and experimental approaches to nuclear clustering, emphasizes recent advances, and examines outstanding questions concerning the structure of ^{9}Be and its significance in nuclear reactions and nucleosynthesis.

1 Introduction

In recent years, nuclear physics has seen rapid progress in studies related to the role of clustering in the structure of exotic nuclei and in the mechanisms governing

their interactions with other nuclei. This trend is evidenced by the large number of experimental and theoretical publications devoted to the manifestation of cluster properties in light exotic nuclei, located near the limits of nucleon stability, as well as by the regular International Conferences on Nuclear Clustering Clustering [1–3].

An illustrative example arises in nucleus–nucleus interactions, where unusual and even unbound nuclear systems may be formed. For instance, in nuclear reactions involving ^{6}He , experimental data have been interpreted as evidence for the existence of a correlated di-neutron pair and a corresponding cluster representation of the ^{6}He nucleus, either as a $(2n + \alpha)$ di-neutron configuration or a so-called "cigar-like" structure [4]. Since the two valence neutrons in ^{6}He may occupy different spatial configurations (di-neutron or cigar-like), the reaction cross section becomes sensitive to the chosen nucleonic arrangement. Thus, elastic scattering observables provide not only the parameters of the optical potential and the interaction radius, but also direct information on the internal structure of ^{6}He and its influence on the underlying reaction mechanism.

Although these measurements suggest sensitivity to neutron correlations, they do not unambiguously confirm the existence of a di-neutron subsystem in ^{6}He . The available data do not align precisely with any single theoretical prediction, and the limited statistics are insufficient to exclude contributions from neutron exchange processes between ^{6}He and ^{4}He at backward angles. Consequently, it has been argued that elastic scattering data for ^{6}He are best compared not only with theoretical models but also with experimental scattering data for its isobar ^{6}Li , measured under identical conditions. Such a comparative approach provides a more direct means to extract structural features of ^{6}He , thereby reducing the ambiguities associated with purely model-dependent interpretations.

Clustering is a well-known phenomenon in light nuclei [5]. Historically, the first evidence for clustering came from the α particle, which, owing to its large binding energy, tends to preserve its identity inside light nuclear systems. The description of nuclear states in terms of cluster substructures was first proposed by Wheeler [6] and Margenau [7], and was later developed into the α-cluster model by Brink and collaborators [8]. This framework has since become one of the most widely applied approaches to explain both the properties of light nuclei and their manifestations in nuclear reactions [7].

A particularly striking example of α clustering is provided by the ^{12}C nucleus and its first excited 0^{+} state at 7.65 MeV, known as the Hoyle state [1, 9]. Modern cluster models predict that this resonance has an anomalously large spatial extension compared to the ground state. The most ambitious interpretation views the Hoyle state as an α-particle Bose–Einstein condensate, in which three nearly unperturbed α particles form a weakly interacting gas-like structure. Such a configuration implies an increase of the nuclear radius by almost a factor of 1.7 relative to the ground state, with direct consequences for the interaction cross sections with other nuclei. This property is of particular astrophysical importance, as it governs the efficiency of the triple-α process and thus the synthesis of ^{12}C in stars.

The nucleon density distributions shown in Fig. 1 [10] illustrate this contrast: the ground state 0_1^{+} exhibits a compact triangular configuration of three α clusters, while the Hoyle state 0_2^{+} reveals an extended, almost linear arrangement. Other low-lying states, such as the 2_1^{+} and 3_1^{-} , retain a triangular geometry, whereas higher excited 0_3^{+} and 2_2^{+} states again display chain-like patterns. These theoretical images

provide a striking visualization of how clustering evolves with excitation energy in ^{12}C, reinforcing the unique role of the Hoyle state in stellar nucleosynthesis.

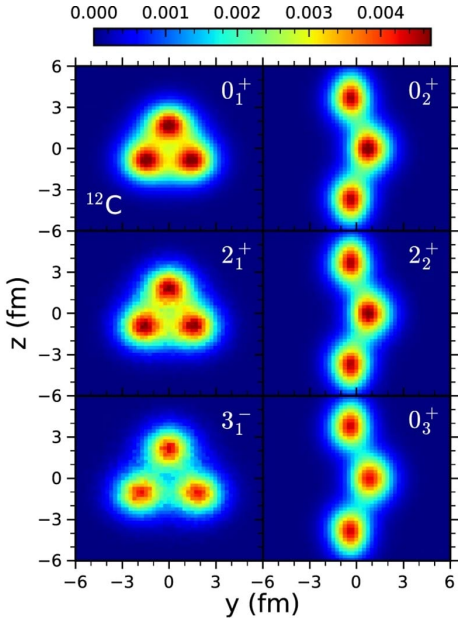

Figure 1: Nucleon density distributions for selected low-lying states of ^{12}C, including the Hoyle state. Triangular configurations characterize the ground (0_1^+) and several excited states, while chain-like structures emerge in the Hoyle state (0_2^+) and higher excitations. Adapted from [10].

Until recently, no experimental method was available to determine the radii of short-lived nuclear states lying above particle-decay thresholds. The introduction of diffraction scattering methods provided a significant breakthrough, offering a way to extract radii of such dilute cluster states [11]. These so-called diffraction radii have since become an important observable for testing microscopic cluster models.

The structure of α-cluster states in light nuclei was first systematized by Ikeda [12], who proposed a diagram illustrating the conditions under which cluster configurations are most likely to occur. The α-cluster picture has since been widely applied to explain the properties of nuclei such as ^{8}Be, ^{12}C, ^{16}O, and others. Comprehensive reviews of recent developments in cluster physics can be found in Refs. [13, 14].

A well-known case is ^{7}Li, which is successfully described within an $\alpha + t$ configuration [15]. In recent years, signatures of clustering have also been observed in nuclei such as ^{16}O, ^{18}O, and ^{19}F. More exotic structures were reported by Freer and co-workers [16], who found evidence for rotational states of a ^{6}He $+^{6}$ He configuration in ^{12}Be. This unusual structure has subsequently been confirmed by different theoretical calculations (see, e.g., Refs. [17, 18]).

An important feature of clustering is that the dominant configuration may change for different excitation energies within the same nucleus [19]. For example, the ground state of ^{5}He is well described as an $\alpha + n$ system, whereas its excited $3/2^+$ state is better represented by a $t + d$ configuration [20]. Thus, as demonstrated by recent studies, many nuclei exhibit α-cluster states at higher excitation energies.

Among the most thoroughly investigated cases are the isotopes of carbon and neon. The 0^+ state at 7.654 MeV in ^{12}C (the Hoyle state) is often interpreted as a chain-like configuration of three α particles. Since this state lies only 0.287 MeV

above the three-α threshold, it plays a key role in both nuclear structure and astrophysical contexts. In Ref. [21], it was shown that in heavier carbon isotopes, deformed "polymeric" chain-like states may be constructed by adding neutrons to the system ($^{12}\mathrm{C}^{*} + xn$).

The isotope $^{15}\mathrm{C}$ contains three valence neutrons, and its isomeric chain-like structure may be interpreted in terms of a $^{10}\mathrm{Be}^{*}$ dimer (itself viewed as $^{9}\mathrm{Be} + n$) coupled with a $^{5}\mathrm{He}$ cluster. For $^{16}\mathrm{C}$, the chain-like configuration can be constructed on the basis of two covalent bonds involving $^{14}\mathrm{C}$ cores. In $^{18}\mathrm{C}$, such chain-like states are expected to be built from $^{11}\mathrm{Be}^{*}$, with three valence neutrons playing the role of covalent bonds. In $^{20}\mathrm{C}$, strongly deformed chain-like states are predicted to arise from excited configurations of $^{12}\mathrm{Be}^{*}$. The population of such highly deformed molecular structures is facilitated when cluster correlations are already present in either the target nuclei or the incident projectiles.

With the development of cluster approaches to nuclear structure, particular attention has been devoted to systems formed by α particles supplemented by valence neutrons. Examples include the isotopes $^{9}\mathrm{Be}$, $^{10}\mathrm{Be}$, $^{10}\mathrm{B}$, and $^{10}\mathrm{C}$, whose cluster structures remain insufficiently explored. These nuclei can be viewed as multi-center molecular configurations in which α particles are linked through covalently bound neutrons. In the simplest case of two α particles, such a system is referred to as a dimer, while for more than two α clusters, the resulting configuration corresponds to a polymer. In either case, the nuclei are strongly deformed, and these cluster states are expected to occur at excitation energies near the thresholds for breakup into the corresponding subsystems.

A possible decay mode of such chain-like states is the emission of reaction fragments [22]. A similar situation is anticipated for the breakup of the $^{9}\mathrm{Be}$ nucleus into clusters. The investigation of the cluster structure of $^{9}\mathrm{Be}$ is therefore of particular interest, and it forms the central focus of the present work.

Collective degrees of freedom, in which groups of several nucleons behave as composite clusters, represent one of the key aspects of nuclear structure. The fundamental building blocks of clustering are the lightest nuclei without excited states, most notably the $^{4}\mathrm{He}$ nucleus (α particle), as well as the deuteron (d), triton (t), and helion ($^{3}\mathrm{He}$). This feature is most clearly manifested in light nuclei, where the number of possible cluster configurations is relatively small. For example, the cluster separation thresholds in nuclei such as $^{7}\mathrm{Be}$, $^{6,7}\mathrm{Li}$, $^{10,11}\mathrm{B}$, $^{11,12}\mathrm{C}$, and $^{16}\mathrm{O}$ lie below the corresponding nucleon separation thresholds. Both the stable nucleus $^{9}\mathrm{Be}$ and the unbound nuclei $^{8}\mathrm{Be}$ and $^{9}\mathrm{B}$ exhibit pronounced cluster structures, and the cluster nuclei $^{7}\mathrm{Be}$, $^{7}\mathrm{Li}$, $^{8}\mathrm{Be}$, and $^{9}\mathrm{B}$ serve as essential building blocks in isotopes such as $^{8}\mathrm{B}$ and $^{9-12}\mathrm{C}$.

Descriptions of the ground states of light nuclei in terms of shell and cluster models are complementary. In the cluster picture, light nuclei are represented as superpositions of various cluster and nucleon configurations. Interest in such states is reinforced by predictions of their molecular-like properties [13,14]. Recent theoretical advances also include the description of the ground states of $^{6,7,9,10}\mathrm{Be}$ using Feynman path-integral techniques, which provide a new perspective on the interplay between collective and single-particle degrees of freedom [23]. Comprehensive reviews of cluster phenomena can be found in Refs. [24,25], which summarize both experimental perspectives and theoretical models.

Traditionally, clustering phenomena have been considered primarily within the

domain of low-energy nuclear reactions [25]. More recently, however, the potential of relativistic nuclear physics has also been recognized for advancing concepts of nuclear clustering. In addition, new concepts of dilute, ultracold nuclear matter have emerged, based on the condensation of nucleons into the lightest nuclei [26–28]. In this context, the α-particle Bose–Einstein condensate has been proposed as a nuclear analogue of atomic quantum gases [29]. These developments highlight the importance of studying diverse cluster ensembles and unbound nuclei as fundamental components of novel quantum media. Coherent cluster ensembles on a macroscopic scale may also play an intermediate role in nucleosynthesis, giving the study of nuclear clustering a significance that extends well beyond nuclear structure itself.

At first glance, the investigation of many-body nuclear systems might appear impossible under laboratory conditions. Nevertheless, such systems can be studied indirectly through breakup processes occurring at excitation energies just above the corresponding thresholds. The configurational overlap of the ground state of a fragmenting nucleus with the final cluster states is fully revealed in peripheral interactions with target nuclei, where the perturbation is minimal. In this sense, the phenomenon of peripheral dissociation of relativistic nuclei may serve as an alternative "laboratory" for probing the unprecedented diversity of cluster ensembles.

The investigation of the ^{9}Be nucleus is of particular importance, as it represents a key system for both few-body nuclear physics and nuclear astrophysics. Its pronounced cluster structure, together with its role as a building block in more complex nuclei, makes ^{9}Be an ideal testing ground for studying the interplay between cluster and single-particle degrees of freedom. Furthermore, understanding the structure and decay properties of ^{9}Be has direct implications for reaction dynamics and for nucleosynthesis pathways in stellar environments. For these reasons, the present work is devoted to a detailed study of the cluster structure of ^{9}Be.

For these reasons, the present work is devoted to a detailed study of the cluster structure of ^{9}Be. Throughout this review we therefore prioritize experimental and theoretical results that directly constrain the competing $^{8}\mathrm{Be} + n$ and $^{5}\mathrm{He} + \alpha$ configurations of ^{9}Be and their astrophysical impact.

2 Structure of the Borromean-stable nucleus ^{9}Be

Although ^{9}Be is a stable nucleus, it is only weakly bound. For instance, the one-neutron separation energy is $S_{1n} = 1.7$ MeV), which is even smaller than the corresponding S_{1n} value in the unstable nucleus ^{6}He [30]. In addition, ^{9}Be exhibits a deformed shape, as reflected in its nuclear quadrupole moment, $Q = +52.9$ mb [31].

Because of these properties, ^{9}Be may be considered as a nucleus with a Borromean structure. This type of configuration is characteristic of weakly bound cluster systems and may, in fact, underlie their stability.

A well-known feature of Borromean nuclei is that none of the two-body subsystems are bound, yet the three-body system as a whole remains stable. In this context, ^{9}Be can be compared with other prominent Borromean systems such as ^{6}He and ^{11}Li. In ^{6}He, the two valence neutrons form correlated di-neutron or “cigar-like” configurations around the α core, while in ^{11}Li, the extreme halo structure arises from two weakly bound neutrons surrounding a ^{9}Li core. In all these cases, the binding is achieved only through the three-body dynamics, and the removal of any constituent immediately leads to an unbound system. Thus, the Borromean character

of ^{9}Be provides an important bridge between stable cluster nuclei and exotic halo systems, linking the physics of light nuclear structure with that of weakly bound and neutron-rich isotopes.

As illustrated in Fig. 2, the structure of ^{9}Be can be represented as an intermediate configuration consisting of two subsystems, one of which is unbound. Accordingly, the possible breakup channels of stable ^{9}Be involve intermediate unbound nuclear systems ^{8}Be and ^{5}He, both of which decay into the final three-body configuration $\alpha + \alpha + n$:

- $^{9}\mathrm{Be} \rightarrow {}^{8}\mathrm{Be} + n \rightarrow \alpha + \alpha + n$,
- $^{9}\mathrm{Be} \rightarrow {}^{5}\mathrm{He} + \alpha \rightarrow \alpha + \alpha + n$,
- $^{9}\mathrm{Be} \rightarrow \alpha + \alpha + n$.

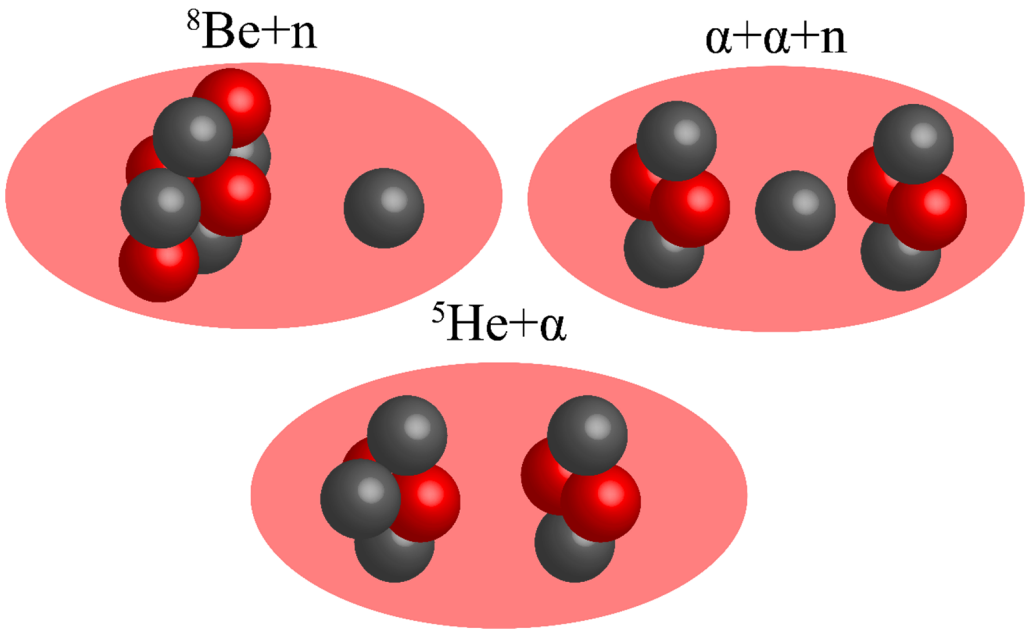

Figure 2: Schematic structural configuration of the ^{9}Be nucleus, illustrating its decay channels through unbound subsystems ^{8}Be and ^{5}He.

Density distributions of the ground states of beryllium isotopes, calculated within the framework of Antisymmetrized Molecular Dynamics (AMD), have been reported in Ref. [32]. These calculations reveal that ^{10}Be can exhibit both symmetric and asymmetric neutron density configurations, whereas ^{9}Be is characterized exclusively by an asymmetric distribution. This asymmetry provides strong evidence for the presence of ^{8}Be and ^{5}He clusters within the ^{9}Be nucleus.

The ^{8}Be system itself is well known as an unbound state consisting of two α particles. Its ground state has often been discussed in the context of an α-particle Bose–Einstein condensate. Such a transition is considered under conditions where fermionic components are absent and additional constraints are met. The addition of a neutron to this α-particle condensate destroys the superfluid-like state, generating instead a binding effect that stabilizes the system. In this way, the structure of ^{9}Be can be viewed as a remarkable example of how a single neutron modifies an otherwise unbound α-cluster configuration, resulting in a Borromean-stable nucleus.

3 Properties of ^{8}Be and ^{12}C and their astrophysical significance

The ^{8}Be nucleus plays a central role in modern astrophysics. As noted above, the most important reaction in stellar helium burning is the so-called triple-α process,

$$^{4}\mathrm{He} + ^{4}\mathrm{He} + ^{4}\mathrm{He} \rightarrow ^{12}\mathrm{C}.$$

The combined energy of three α particles is 7.28 MeV above the rest energy of the ^{12}C nucleus. For this reaction to proceed efficiently, a suitable resonant level in ^{12}C must exist. Indeed, such a state is available: the famous Hoyle state at 7.656 MeV. As a result, the triple-α reaction in stars occurs with sufficient rate to produce carbon, making this resonance one of the cornerstones of stellar nucleosynthesis.

The first step involves the fusion of two α particles to form the short-lived nucleus ^{8}Be, via

$$^{4}\mathrm{He} + ^{4}\mathrm{He} \rightarrow ^{8}\mathrm{Be}.$$

Although the lifetime of ^{8}Be is only about 10^{-16} s, there remains a finite probability that an additional α particle will be captured, leading to the excited ^{12}C nucleus:

$$^{8}\mathrm{Be} + ^{4}\mathrm{He} \rightarrow ^{12}\mathrm{C}^{*}.$$

The de-excitation of $^{12}\mathrm{C}^{*}$ occurs not through γ emission, which is forbidden by selection rules, but rather through the creation of an $e^{+}e^{-}$ pair:

$$^{12}\mathrm{C}^{*} \rightarrow ^{12}\mathrm{C} + e^{+} + e^{-}.$$

It should be noted that the $^{12}\mathrm{C}^{*}$ nucleus most often decays back into $^{8}\mathrm{Be} + ^{4}\mathrm{He}$ and eventually into three α particles. Only in about one out of every 2500 cases does the system instead decay to the ground state, releasing the 7.65 MeV excitation energy via pair emission. This extremely rare but crucial transition underpins the cosmic abundance of carbon and highlights the delicate interplay between nuclear structure and astrophysical processes.

Another possible cluster component of ^{9}Be is ^{5}He. In contrast to ^{8}Be, the ^{5}He system is even more diffuse and unstable, with a lifetime of about 7×10^{-22} s, compared to 8×10^{-17} s for ^{8}Be. This difference of five orders of magnitude in lifetime raises doubts regarding the existence of a well-defined ^{5}He cluster inside ^{9}Be.

From a structural perspective, the comparison between ^{8}Be and ^{5}He emphasizes the unique role played by near-threshold resonances in cluster physics. While the fleeting existence of ^{8}Be enables it to act as an essential stepping stone in the triple-α process, the even shorter lifetime of ^{5}He strongly limits its relevance as a constituent cluster in stable nuclei. Nevertheless, the possible contribution of ^{5}He-like correlations to the structure of ^{9}Be cannot be entirely excluded, and remains an open topic of theoretical and experimental investigation.

4 Cluster structure of ^{9}Be

This section summarizes experimental evidence for cluster channels, classification schemes, and transfer-reaction studies.

The structure of ^{9}Be has been extensively studied in a variety of experimental works [33–40, 42]. These studies have identified the dominant breakup channels of ^{9}Be as $^{8}\mathrm{Be}_{\mathrm{g.s.},2^+} + n$ and $^{5}\mathrm{He} + \alpha$. Despite the weakly bound nature of ^{5}He, it has been shown that the decay of higher-lying states in ^{9}Be ($E > 4$ MeV) proceeds predominantly through the $^{5}\mathrm{He}_{\mathrm{g.s.}}$ channel. Table 1 summarizes the relevant levels of ^{9}Be and the associated ^{5}He cluster configurations.

Table 1: Decay channels of selected excited states of ^{9}Be with their registration efficiency and branching ratios.

E_x (^{9}Be, MeV)	Decay channel	Detection efficiency	Branching ratio (%)
1.684	$^{8}\mathrm{Be}_{\mathrm{g.s.}}$	0.5	100
	$^{8}\mathrm{Be}_{2^+}$	2.8	0
2.43	$^{8}\mathrm{Be}_{\mathrm{g.s.}}$	3.5	6 ± 1
	$^{8}\mathrm{Be}_{2^+}$	2.5	94 ± 2
	$^{5}\mathrm{He}_{\mathrm{g.s.}}$	2.7	< 5
6.3–6.85	$^{8}\mathrm{Be}_{\mathrm{g.s.}}$	3.2	4 ± 1
	$^{8}\mathrm{Be}_{2^+}$	1.1	7 ± 3
	$^{5}\mathrm{He}_{\mathrm{g.s.}}$	3.2	89 ± 35
11.1–11.5	$^{8}\mathrm{Be}_{\mathrm{g.s.}}$	3.2	3 ± 1
	$^{8}\mathrm{Be}_{2^+}$	1.1	21 ± 8
	$^{5}\mathrm{He}_{\mathrm{g.s.}}$	0.2	76 ± 30

As seen from Table 1, these reaction channels are of considerable astrophysical importance. The presence of a ^{5}He cluster can significantly alter the accepted scheme of nucleosynthesis involving ^{9}Be. The formalism presented in Ref. [36] for deriving the $\alpha\alpha n$ reaction rate suggested that broad intermediate resonances would have only a minor impact. However, more recent theoretical calculations have demonstrated that at temperatures above 3×10^{9} K the ^{5}He channel becomes important for the formation of ^{9}Be [37]. Together with the qualitative decay patterns discussed above, these results strongly indicate the need for quantitative data on the branching ratios of low-lying ^{9}Be states.

As noted in Ref. [34], higher-lying levels in ^{9}Be decay mainly through the ^{5}He cluster, while the lower-lying states decay preferentially via ^{8}Be. Thus, the structure of ^{9}Be appears to be governed by a multicluster configuration in both the ground and excited states.

Further insights were obtained in Ref. [42], where angular distributions were measured for transitions to the ground states of ^{5}He and ^{6}Li, as well as to the excited states of ^{6}Li at 2.185 MeV (3^+), 5.37 MeV (2^+), and 5.65 MeV (1^+). These measurements were performed for the reactions $^{9}\mathrm{Be}(^{3}\mathrm{He},^{8}\mathrm{Be})\alpha$ and $^{9}\mathrm{Be}(^{3}\mathrm{He},^{6}\mathrm{Li})^{6}\mathrm{Li}$ at an incident energy of 60 MeV. The experimental data were analyzed within the coupled-channel method, including one- and two-step cluster transfers, as well as cluster spectroscopic amplitudes calculated in the framework of the translationally invariant shell model. It was found that coupling to inelastic channels and reorientation effects significantly modified the elastic scattering cross sections at large angles and allowed for a satisfactory description of the data. In contrast, direct cluster transfer processes were found to play only a minor role.

In Ref. [43], the population of excited states in ^{9}Be up to $E_x = 8$ MeV was measured in the $^{9}\mathrm{Be}(\alpha, 3\alpha)n$ reaction at beam energies of 22 and 26 MeV. A new level was identified at $E_x = 3.82^{+0.08}_{-0.09}$ MeV with a width of $\Gamma = 1240^{+270}_{-90}$ keV. The reduced width of this state in the $^{8}\mathrm{Be}_{\mathrm{g.s.}}$ channel, compared to the mirror nucleus ^{9}B, suggested spin-parity assignments of $J^{\pi} = (1/2)^{-}$ or $(3/2)^{-}$.

Further insight into the classification of ^{9}Be states was provided in Ref. [44], where the correspondence between the observed levels and Young tableaux $\{42\}$ and $\{43\}$ was established within a multicluster shell model. Possible configurations such as $\alpha\alpha n$ and αtd were considered within cluster models. It was shown that while the three-body $\alpha\alpha n$ description naturally reproduces channels involving neutrons, protons, deuterons, tritons, and α particles, the αtd configuration does not predict neutron emission. This discrepancy is consistent with the observation that neutron emission accompanies the formation of the ground and first excited states of ^{8}Be, whose wave functions correspond to the $\{43\}$ Young scheme. Therefore, states of αtd nature in ^{9}Be are likely to appear predominantly at higher excitation energies. The simultaneous observation of α emission provides additional evidence for the presence of ^{5}He clusters in ^{9}Be.

An independent experimental approach was employed in Ref. [45], where nuclear emulsions were used to directly register cluster fragments. These measurements supported a structural picture of ^{9}Be consisting primarily of a ^{8}Be core (in both 0^{+} and 2^{+} configurations with approximately equal weights) plus a valence neutron (Fig. 3). However, due to the limitations of the emulsion method, signatures of $^{5}\mathrm{He} + \alpha$ channels could not be resolved. Thus, while the $^{8}\mathrm{Be} + n$ structure was firmly established, further clarification of the ^{5}He contribution requires the use of modern semiconductor detector systems with on-line data acquisition, which provide the necessary resolution and efficiency.

An important result was obtained in Refs. [46, 47], where the radii of low-lying excited states in ^{9}Be were determined. In these studies, differential cross sections for inelastic scattering were measured, providing access to rms radii of short-lived states in stable nuclei such as ^{13}C and ^{9}Be. In addition, the radioactive nucleus ^{11}Be was found to exhibit an anomalously large rms radius for its low-lying states, interpreted as evidence of a neutron halo. More detailed and systematic information on charge radii across the Be isotopic chain was later obtained by high-precision laser spectroscopy in Ref. [48].

These measurements are of particular importance for cluster physics, as they provide one of the few experimental probes of spatial extensions of short-lived states above decay thresholds. For ^{9}Be, the results demonstrate that clustering effects manifest not only in the decay patterns but also in the geometric properties of excited configurations. The comparison with ^{11}Be highlights a smooth transition between ordinary cluster structures and genuine halo phenomena, thus linking the study of stable cluster nuclei with the frontier of exotic nuclear structure.

The results of these studies allow one to trace the evolution of nuclear radii in Be isotopes as a function of neutron number. The maximum radius is observed for ^{7}Be, which can be explained by its cluster structure ($^{4}\mathrm{He} + ^{3}\mathrm{He}$). With the addition of neutrons, the nuclear radius decreases, reaching a minimum for the isotopes ^{9,10}Be. These nuclei are well described by a $2\alpha + n_x$ cluster configuration. Interestingly, the rms radius of the radioactive nucleus ^{10}Be is smaller than that of the stable nucleus ^{9}Be, a feature that may be attributed to neutron pairing effects. This observation

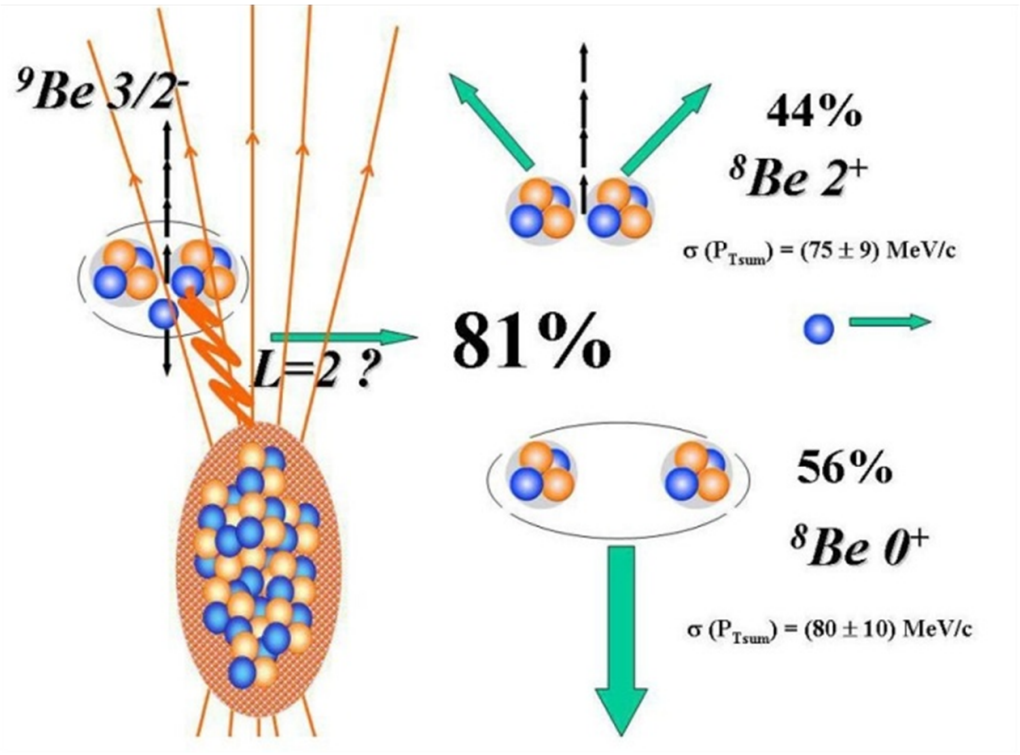

Figure 3: Schematic illustration of the dissociation of ^{9}Be into $^{8}\mathrm{Be} + n$, based on the cluster-emulsion study of Ref. [45].

underscores the importance of detailed investigations into the internal structure of ^{9,10}Be.

The possible existence of a ^{5}He cluster within ^{9}Be was first discussed in Ref. [40]. In that work, angular distributions of protons, deuterons, tritons, and α particles emitted from $d + ^{9}$Be reactions at $E_d = 7$ MeV were measured, together with excitation functions in the range $E_{\mathrm{lab}} = 6.5$–7.5 MeV at selected angles. The elastic scattering potential was described within a phenomenological optical model, while compound-nucleus contributions in all outgoing channels were evaluated using the Hauser–Feshbach formalism and found to be at most 10–20%. To minimize such compound contributions, subsequent studies—including the present work—employed higher beam energies.

It is also important to note that Ref. [40] considered the role of sequential versus simultaneous nucleon transfer mechanisms. In particular, the collective excitation of the $E_x = 2.43$ MeV state in ^{9}Be and nucleon transfer processes were analyzed within the distorted-wave Born approximation (DWBA). The results indicated a significant contribution from the transfer of five nucleons as a single correlated cluster in the (d, α) channel, thereby providing early evidence for multicluster dynamics in ^{9}Be.

In Ref. [49], angular distributions for the $^{12}\mathrm{C}(^{11}\mathrm{B},^{6}\mathrm{Li})^{17}\mathrm{O}$ reaction were measured at beam energies of 28, 35, and 40 MeV. The data were analyzed within the finite-range distorted-wave Born approximation (DWBA), including both first- and second-order processes, under the assumption of simultaneous and sequential transfer of a neutron and an α particle. A similar analysis was also applied to previously measured angular distributions of the $^{12}\mathrm{C}(d,^{7}\mathrm{Li})^{7}\mathrm{Be}$ reaction at $E_{\mathrm{lab}} = 78$ MeV [50]. In both

cases, the results indicated a dominance of the simultaneous transfer of an α particle and a correlated nucleon, consistent with the presence of a ^{5}He (^{5}Li) cluster in either the ground or first excited state.

These conclusions, however, stand in contrast to the findings of Ref. [42], where it was argued that sequential nucleon transfer constitutes the dominant mechanism. In that study, the ^{9}Be(^{3}He,^{4}He)^{8}Be reaction was included to constrain the optical potential for the intermediate ^{4}He+^{8}Be channel in two-step transfer processes. The analysis revealed that in the ^{9}Be(^{3}He,^{7}Be)^{5}He reaction, α transfer dominates only at small angles, whereas two-neutron transfer becomes important at larger angles. In the angular range $\theta \approx 30^{\circ} - 80^{\circ}$, the cross sections were primarily governed by sequential transfer of a neutron and a ^{3}He cluster, as well as by the transfer of two deuterons. Transitions through highly excited intermediate states of ^{8}Be and ^{7}Li were also found to contribute substantially to the measured cross sections.

Similarly, in the ^{9}Be(^{3}He,^{6}Li)^{6}Li reaction, triton transfer was found to dominate only for transitions to excited states of ^{6}Li, while the cross section for transitions to the ^{6}Li ground state was primarily described by sequential transfer of a neutron and a deuteron.

These contrasting interpretations highlight the complexity of cluster-transfer mechanisms in weakly bound nuclei. They underscore the necessity for further experimental studies aimed at identifying clusters in light, weakly bound systems, including exotic unbound clusters such as $2n$, ^{5}H, ^{8}Be, and ^{5}He. The presence of such cluster configurations may manifest in reactions with both light and heavy ions, leaving distinctive signatures in the observables. The intrinsic three-body nature of weakly bound nuclei further complicates theoretical descriptions, calling for refined models that can simultaneously account for direct, sequential, and correlated cluster-transfer processes.

5 Recent experimental advances

Beyond the studies summarized above, several post-2016 experiments have sharpened constraints on clustering in ^{9}Be and neighboring systems. Recent work, such as the 2025 study of α-clustering in ^{9}Be through complete fusion and elastic scattering, has refined level assignments and partial widths in the low-energy regime [51]. Advances in direct-reaction techniques using active-target TPCs (e.g. “Direct reactions with the AT-TPC”) enable high-resolution studies of cluster states, even when only low-intensity beams are available [52]. Meanwhile, the development of new detectors, such as the Fudan Multi-purpose Active Target Time Projection Chamber, expands the experimental capabilities for photonuclear and α-cluster studies [53]. Recent reviews of clustering progress (e.g. “Clustering in nuclei: progress and perspectives”) place these experimental advances in a broader context [54]. In addition, reviews of detector strategies for quasi-free scattering (2024) further underscore the rapid evolution of the experimental toolkit [55]. Together, these developments reduce model ambiguities in disentangling the competing cluster configurations of ^{9}Be that are most relevant for astrophysical reaction networks.

6 Role of ^{9}Be clustering in nucleosynthesis

The ^{9}Be nucleus plays a crucial role in astrophysical nucleosynthesis. At present, there is no fully adequate explanation for its observed abundance in the Universe. Several works [56–58] have demonstrated the importance of ^{9}Be in r-process scenarios in the light-mass region. In particular, reliable cross-section data for reactions such as

$$^{8}\mathrm{Be}(n,\gamma)^{9}\mathrm{Be} \quad \text{and} \quad ^{9}\mathrm{Be}(\gamma,n)^{8}\mathrm{Be}$$

are essential for modeling reaction chains in the r process. These reactions directly impact the possible synthesis of ^{12}C under neutron-rich astrophysical conditions.

6.1 Connection to the triple-α process

The classical triple-α process proceeds via the short-lived ^{8}Be nucleus as an intermediate step. Although the lifetime of ^{8}Be is only $\sim 10^{-16}$ s, it allows for the capture of a third α particle, producing the Hoyle state in ^{12}C [9]. This resonance strongly enhances the synthesis of carbon in stars, thereby determining the efficiency of stellar helium burning.

Cluster correlations in ^{9}Be influence this mechanism indirectly, because they provide competing reaction pathways and modify the reaction flow toward ^{12}C. In particular, near-threshold states of ^{9}Be, such as the $1/2^{+}$ resonance, play an important role in the alternative reaction chain

$$^{8}\mathrm{Be}(n,\gamma)^{9}\mathrm{Be}(\alpha,n)^{12}\mathrm{C},$$

which may complement or even compete with the standard triple-α process under neutron-rich astrophysical conditions [56–58]. This highlights the dual role of ^{9}Be: while not directly part of the triple-α mechanism, it serves as a bridge nucleus in neutron-enriched environments, influencing the efficiency of ^{12}C production in r-process scenarios.

Moreover, theoretical studies [36,37] suggest that the existence of cluster configurations such as $^{5}\mathrm{He}+\alpha$ could open additional channels for ^{9}Be formation. Although the lifetime of ^{5}He is extremely short ($\sim 10^{-21}$ s), at sufficiently high temperatures and densities its transient existence can contribute to reaction pathways that bypass the fragile ^{8}Be resonance. These alternative cluster-driven mechanisms remain the subject of active research, as they may substantially affect nucleosynthesis yields in explosive astrophysical environments such as supernovae and neutron star mergers.

Taken together, the interplay between the classical triple-α reaction and the cluster-influenced pathways involving ^{9}Be underscores the importance of precise nuclear-structure information. Accurate cross-section measurements and improved theoretical models are essential for constraining the role of ^{9}Be in both helium burning and r-process nucleosynthesis.

6.2 Alternative r-process pathways through unbound clusters

In addition to the triple-α route, theoretical calculations [37] suggest that at temperatures $T \sim 10^{9}$ K, ^{9}Be may also form via an intermediate unbound ^{5}He cluster.

Such a mechanism would open an alternative reaction channel:

$$^{4}\mathrm{He}(n,\gamma)^{5}\mathrm{He}(\alpha,\gamma)^{9}\mathrm{Be},$$

which competes with the standard path

$$^{8}\mathrm{Be}(n,\gamma)^{9}\mathrm{Be}.$$

The existence of this alternative channel highlights the possible role of unstable cluster states in stellar nucleosynthesis. A schematic of this extended network, including both the ^{5}He- and ^{8}Be-based routes, is shown in Fig. 4.

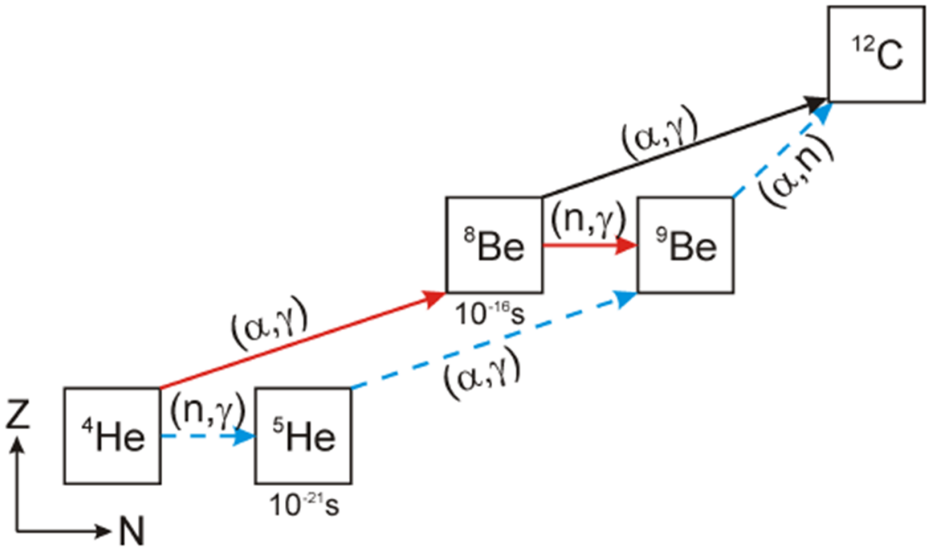

Figure 4: Alternative nucleosynthesis pathways for ^{9}Be formation. The classical triple-α process proceeds through ^{8}Be and the Hoyle state in ^{12}C (red arrows), while an alternative scenario involves the unbound ^{5}He cluster (blue dashed arrows).

7 Modern directions and open questions

The study of clustering in light nuclei continues to evolve rapidly, with several modern directions and unresolved problems attracting particular attention.

7.1 Prospects for studying clustering in exotic nuclei

One of the most important future directions is the investigation of clustering in exotic nuclei near the drip lines. Neutron-rich systems such as ^{11}Li, ^{14}Be, and ^{17}B, as well as proton-rich nuclei like ^{8}B, provide unique laboratories for testing cluster correlations under extreme conditions of isospin asymmetry. These nuclei often exhibit halo or Borromean features, where clusterization becomes intertwined with weak binding and continuum effects [13, 14, 32]. Understanding their structures requires a combined description in terms of both cluster and shell-model components, highlighting the challenge of unifying different theoretical frameworks.

7.2 Role of high-energy experiments and new detection techniques

Progress in the field is increasingly driven by high-energy experiments at radioactive-ion beam facilities. Breakup and transfer reactions at intermediate and relativistic energies allow one to probe cluster configurations through momentum distributions and correlations between fragments [43, 45]. New experimental techniques, such as active-target detectors, advanced γ-ray tracking arrays, and high-resolution recoil separators, provide unprecedented sensitivity to rare reaction channels and short-lived cluster states [59, 60]. In particular, the combination of high-luminosity beams and modern detector systems operating in on-line mode enables detailed spectroscopy of unbound nuclei and precise determination of branching ratios in competing cluster decay modes.

7.3 Weakly bound and many-body systems as a test for nuclear models

Weakly bound nuclei, especially Borromean systems, represent a stringent test for theoretical models of nuclear structure and reactions. In such systems, none of the binary subsystems are bound, and stability arises only due to three-body correlations. This requires theoretical approaches capable of simultaneously treating continuum dynamics, nucleon correlations, and cluster degrees of freedom. Methods such as antisymmetrized molecular dynamics (AMD) [32], the no-core shell model with continuum (NCSMC), and complex-scaling approaches have provided valuable insights, yet significant discrepancies remain when comparing with experimental data [36, 58].

The description of multicluster ensembles and dilute nuclear states, such as the Hoyle state in ^{12}C, also remains an open challenge. Interpretations in terms of α-particle Bose–Einstein condensation [28, 29] have stimulated active discussions about the limits of clustering and its role in astrophysical nucleosynthesis.

Overall, the field of nuclear clustering stands at the intersection of structure, reactions, and astrophysics. Further advances will depend on the synergy of high-precision experiments, large-scale theoretical calculations, and cross-disciplinary approaches, including analogies with quantum gases and condensed-matter systems.

Practical implications. For applications to network calculations we emphasize: (i) the need for updated partial widths and branching ratios of near-threshold ^{9}Be states; (ii) consistent treatment of $^{8}\mathrm{Be} + n$ vs. $^{5}\mathrm{He} + \alpha$ formation paths in stellar conditions; and (iii) radius-sensitive observables that benchmark models used to extrapolate reaction rates beyond measured windows.

8 Conclusion

The ^{9}Be nucleus represents a weakly bound Borromean system where $^{8}\mathrm{Be} + n$ and $^{5}\mathrm{He} + \alpha$ configurations govern its structure and decay properties. These cluster degrees of freedom are observed in decay, transfer, and scattering processes, with direct implications for nucleosynthesis, including alternative pathways to the triple-α and r-processes.

Open issues include the quantitative role of ^{5}He-like correlations, branching ratios of low-lying states, and the influence of near-threshold resonances under astrophysical conditions. Progress in active-target detection, γ-ray tracking, and recoil spectroscopy, together with microscopic cluster and many-body models, is essential to constrain these aspects.

Thus, ^{9}Be remains a key test case for exploring the interplay of cluster and single-particle dynamics and for evaluating its contribution to element synthesis in the Universe.

References

[1] Yu.E. Penionzhkevich, R.G. Kalpakchieva, Light Nuclei at the Boundary of Neutron Stability (JINR, Dubna, 2016), 383 p.

[2] *12th International Conference on Clustering Aspects of Nuclear Structure and Dynamics (CLUSTER'22 → held in 2023)*, Dubna, Russia, 20–24 June 2023. Indico page: `https://indico.jinr.ru/event/1026/`. (Accessed Sep 25, 2025).

[3] *Clusters'26: 12th International Conference on Clustering Aspects of Nuclear Structure and Dynamics*, Institute of Physics, London, UK (upcoming). Conference website: `https://iop.eventsair.com/clusters26/`. (Accessed Sep 25, 2025).

[4] G.M. Ter-Akopian, A.M. Rodin, A.S. Fomichev *et al.*, Phys. Lett. B **426**, 251 (1998).

[5] D.M. Brink, J. Phys.: Conf. Ser. **111**, 012001 (2008).

[6] J.A. Wheeler, Phys. Rev. **52**, 1083 (1937).

[7] H. Margenau, Phys. Rev. **59**, 37 (1941).

[8] D. Brink, J.J. Castro, Nucl. Phys. A **216**, 109 (1973).

[9] F. Hoyle, Astrophys. J. Suppl. **1**, 121 (1954).

[10] S. Shen, S. Elhatisari, T.A. Lähde, D. Lee, B.-N. Lu, U.-G. Meißner, Nat. Commun. **14**, 2777 (2023).

[11] A.S. Demyanova, A.A. Ogloblin, S.A. Goncharov, T.L. Belyaeva, J. Mod. Phys. E **17**, 2118 (2008).

[12] K. Ikeda, N. Takigawa, H. Horiuchi, Prog. Theor. Phys. Suppl. **E68**, 464 (1968).

[13] W. von Oertzen, M. Freer, Y. Kanada-En'yo, Phys. Rep. **432**, 43 (2006).

[14] M. Freer, Rep. Prog. Phys. **70**, 2149 (2007).

[15] Y. Fujiwara, Y.C. Tang, Phys. Rev. C **31**, 342 (1985).

[16] M. Freer, J.C. Angélique, L. Axelsson *et al.*, Phys. Rev. Lett. **82**, 1383 (1999).

[17] P. Descouvemont, D. Baye, Phys. Lett. B **505**, 71 (2001).

[18] M. Dufour, P. Descouvemont, F. Nowacki, Nucl. Phys. A **836**, 242 (2010).

[19] K. Wildermuth, T. Kanellopoulos, Nucl. Phys. **9**, 449 (1958).

[20] Y.C. Tang, Lect. Notes Phys. **145**, 571 (1981).

[21] W. von Oertzen, Acta Phys. Pol. B **29**, 247 (1998).

[22] R.G. Kalpakchieva, Yu.E. Penionzhkevich, Phys. Elem. Part. At. Nucl. **33**, 1247 (2002).

[23] V.V. Samarin, Izv. RAN **84**(8), 1187 (2020).

[24] A. Pakou, O. Sgouros, V. Soukeras *et al.*, Phys. Rev. C **101**, 024602 (2020).

[25] P. Papka, C. Beck, Lect. Notes Phys. **2**, 299 (2012).

[26] C.J. Horowitz, M.A. Pérez-García, D.K. Berry, J. Piekarewicz, Phys. Rev. C **72**, 035801 (2005).

[27] S. Shlomo, G. Röpke, J.B. Natowitz *et al.*, Phys. Rev. C **79**, 034604 (2009).

[28] T. Yamada, Y. Funaki, H. Horiuchi *et al.*, Lect. Notes Phys. **848**, 229 (2012).

[29] D. Baye, P. Capel, Lect. Notes Phys. **848**, 121 (2012).

[30] M. Wang, G. Audi, A.H. Wapstra *et al.*, Chin. Phys. C **36**(12), 1603 (2012).

[31] D. Sundholm, J. Olsen, Chem. Phys. Lett. **177**(1), 91 (1991).

[32] Y. Kanada-En'yo, M. Kimura, H. Horiuchi, C. R. Physique **4**, 497 (2003).

[33] T.A.D. Brown, P. Papka, B.R. Fulton *et al.*, Phys. Rev. C **76**, 054605 (2007).

[34] P. Papka, T.A.D. Brown, B.R. Fulton *et al.*, Phys. Rev. C **75**, 045803 (2007).

[35] R. Bansal, S. Gautam, R.K. Puri *et al.*, J. Phys. G: Nucl. Part. Phys. **41**, 035103 (2014).

[36] L.V. Grigorenko, M.V. Zhukov, Phys. Rev. C **72**, 015803 (2005).

[37] L. Buchmann, Phys. Rev. C **64**, 022801 (2001).

[38] C. Détraz, H.H. Duhm, H. Hafner, Nucl. Phys. A **147**(3), 488 (1970).

[39] C. Détraz, F. Pougheon, M. Bernas *et al.*, Nucl. Phys. A **228**(1), 39 (1974).

[40] A. Szczurek, K. Bodek, J. Krug *et al.*, Z. Phys. A **333**, 271 (1989).

[41] V. Zagrebaev, A. Denikin, A. Alekseev, DWBA for Nucleon Transfer Reactions, available at: `http://nrv.jinr.ru/` (2020).

[42] A.T. Rudchik, E.I. Koshchy, A. Budzanowski *et al.*, Nucl. Phys. A **609**(2), 147 (1996).

[43] R. Smith, C. Wheldon, M. Freer *et al.*, Phys. Rev. C **94**, 014320 (2016).

[44] M.A. Zhusupov, R.S. Kabatayeva, Bull. Rus. Acad. Sci. Phys. **76**, 429 (2012).

[45] P.I. Zarubin, Lecture Notes in Physics **3**, 51 (2014).

[46] A.A. Ogloblin, A.N. Danilov, T.L. Belyaeva *et al.*, Phys. Rev. C **84**, 054601 (2011).

[47] A.S. Demyanova, A.A. Ogloblin, A.N. Danilov *et al.*, Proc. Int. Symp. on Exotic Nuclei (EXON 2012), Vladivostok, p.83 (2012).

[48] W. Nörtershäuser, D. Tiedemann, M. Žáková, Z. Andjelkovic *et al.*, Phys. Rev. Lett. **102**, 062503 (2009).

[49] L. Jarczyk, B. Kamys, M. Kistryn *et al.*, Phys. Rev. C **54**, 1302 (1996).

[50] L. Jarczyk, B. Kamys, B. Styczen *et al.*, Z. Phys. A **325**, 303 (1986).

[51] A. Kundu, S. Bhattacharya, A. Saxena *et al.*, Phys. Lett. B **864**, 139441 (2025).

[52] Y. Ayyad, D. Bazin, F. Bonaiti, J. Chen *et al.*, Front. Phys. **13**, 1539148 (2025).

[53] H.-K. Wu, X.-Y. Wang, Y.-M. Wang *et al.*, arXiv:2406.18599 [physics.ins-det] (2024).

[54] K. Wei, Y.-L. Ye, Z.-H. Yang, Nucl. Sci. Tech. **35**, 216 (2024).

[55] J. Tanaka, M.L. Cortes, H. Liu, R. Taniuchi *et al.*, arXiv:2412.17887 [physics.ins-det] (2024).

[56] C.W. Arnold, T.B. Clegg, C. Iliadis *et al.*, Phys. Rev. C **85**, 044605 (2012).

[57] O. Burda, P. von Neumann-Cosel, A. Richter, C. Forssén, B.A. Brown, Phys. Rev. C **82**, 015808 (2010).

[58] J. Casal, M. Rodriguez-Gallardo, J.M. Arias, I.J. Thompson, Phys. Rev. C **90**, 044304 (2014).

[59] W.H. Trzaska *et al.*, Nucl. Instrum. Meth. A **903**, 241 (2018).

[60] B. Cheal, D.H. Forest, Hyperfine Interactions **223**, 63 (2014).